# Structural Details on the Binding of Antihypertensive Drugs Captopril and Enalaprilat to Human Testicular Angiotensin I-Converting Enzyme[†,‡]

Ramanathan Natesh,[§,||] Sylva L. U. Schwager,[⊥] Hazel R. Evans,[§] Edward D. Sturrock,*[,⊥] and K. Ravi Acharya*[,§]

*Department of Biology and Biochemistry, University of Bath, Claverton Down, Bath BA2 7AY, United Kingdom, and Division of Medical Biochemistry and Institute of Infectious Disease and Molecular Medicine, University of Cape Town, Observatory 7925, South Africa*

*Received March 16, 2004; Revised Manuscript Received May 10, 2004*

ABSTRACT: Angiotensin converting enzyme (ACE) plays a critical role in the circulating or endocrine renin−angiotensin system (RAS) as well as the local regulation that exists in tissues such as the myocardium and skeletal muscle. Here we report the high-resolution crystal structures of testis ACE (tACE) in complex with the first successfully designed ACE inhibitor captopril and enalaprilat, the Phe-Ala-Pro analogue. We have compared these structures with the recently reported structure of a tACE−lisinopril complex [Natesh et al. (2003) *Nature 421*, 551−554]. The analyses reveal that all three inhibitors make direct interactions with the catalytic $Zn^{2+}$ ion at the active site of the enzyme: the thiol group of captopril and the carboxylate group of enalaprilat and lisinopril. Subtle differences are also observed at other regions of the binding pocket. These are compared with N-domain models and discussed with reference to published biochemical data. The chloride coordination geometries of the three structures are discussed and compared with other ACE analogues. It is anticipated that the molecular details provided by these structures will be used to improve the binding and/or the design of new, more potent domain-specific inhibitors of ACE that could serve as new generation antihypertensive drugs.

Angiotensin I-converting enzyme (ACE,[1] EC 3.4.15.1) is a zinc metallopeptidase that has received considerable attention because of its pivotal role in blood pressure regulation by catalyzing the proteolysis of angiotensin I to the vasopressor angiotensin II (*2*−*5*). ACE inhibitors are widely used to treat cardiovascular diseases, including high blood pressure, heart failure, coronary artery disease, and kidney failure. There are two isoforms of ACE: in somatic tissues, it exists as a glycoprotein composed of a single large polypeptide chain of 1277 amino acids; in germinal cells, it is synthesized as a lower molecular mass form and is thought to play a role in sperm maturation and the binding of sperm to the oviduct epithelium (*6*). Somatic ACE is composed of functionally active N- and C-domains resulting from tandem gene duplication. Despite the high degree of sequence similarity between the two domains, they differ in both substrate and inhibitor specificity and chloride activation. The C domain is primarily involved in blood pressure regulation (reviewed in ref *5*), whereas the N domain is far more specific for the hemoregulatory tetrapeptide AcSDKP, which controls hematopoietic stem cell differentiation and proliferation (*7*). More recently, the use of two potent domain-specific phosphinic peptide inhibitors, RXP407 (N domain) and RXPA380 (C domain), demonstrated that the selective inhibition of only one of the two domains in vivo prevented hydrolysis of angiotensin I (*8*). However, inhibition of both active sites was necessary to abrogate the conversion of bradykinin to its inactive product. Furthermore, mice homozygous for a mutation inactivating the N domain, but not the C domain, of somatic ACE retained a phenotype indistinguishable from that of wild-type mice with regard to blood pressure and renal function (*9*). Thus, inhibition of one domain (C domain) may be necessary and sufficient for the treatment of certain cardiorenal diseases.

Due to the critical role of ACE in cardiovascular and renal diseases, it has been an attractive target for drug design. The development of captopril, the first marketed orally active ACE inhibitor approved for treatment of human hypertension, was accomplished in 1981 by Cushman and Ondetti and co-workers (*10*−*12*) based on three key features of the enzyme. First, ACE was thought to be a carboxypeptidase that catalyzed the hydrolysis of dipeptides from the C-terminus of oligopeptides. In addition, it was inhibited by chelating agents and could be reactivated by zinc and other divalent cations. In this regard it resembled the much better characterized enzyme carboxypeptidase A from bovine pancreas (an enzyme found in the digestive system of all mammals),

[†] This work was supported by the Wellcome Trust U.K. (Project Grant 071047 to K.R.A., a Senior International Research Fellowship 070060 to E.D.S.) and the National Research Foundation, South Africa (grant to E.D.S.).

[‡] The atomic coordinates have been deposited with the Protein Data Bank, www.rcsb.org, and the accession codes are 1UZE and 1UZF for the enalaprilat and captopril complexes, respectively.

* To whom correspondence should be addressed. Tel: +44-1225-386238; Fax: +44-1225-386779; e-mail Sturrock@curie.uct.ac.za or K. R.Acharya@bath.ac.uk.

[§] University of Bath.

[||] Present address: ICGEB, New Delhi, India.

[⊥] University of Cape Town.

[1] Abbreviations: ACE, angiotensin I-converting enzyme; tACE, human testicular angiotensin I-converting enzyme; AnCE, *Drosophila* homologue of angiotensin I-converting enzyme; HEPES, *N*-(2-hydroxyethyl)piperazine-*N*′-2-ethanesulfonic acid; PEG, poly(ethylene glycol); PMSF, phenylmethanesulfonyl fluoride.

10.1021/bi049480n CCC: $27.50 
Published on Web 06/18/2004

Table 1: N- and C-Selectivity of Known Small Molecule ACE Inhibitors

| | residues[b] | | | domain inhibition[a] (nM) | | | |
|---|---|---|---|---|---|---|---|
| | | | | N domain | | C domain | |
| inhibitor | $P_1$ | $P_1'$ | $P_2'$ | 20 mM NaCl | 300 mM NaCl | 20 mM NaCl | 300 mM NaCl |
| captopril | | Ala | Pro | 9.1 | 8.9 | 111 | 14 |
| enalapril | Phe | Ala | Pro | 31 | 26 | 78 | 6.3 |
| lisinopril | Phe | Lys | Pro | 42 | 44 | 27 | 2.4 |

[a] Determined as $K_i$ with Hip-His-Leu as a substrate in every case (*24*). [b] C-terminal amino acid residues of small-molecule ACE inhibitors (captopril, enalapril and lisinopril).

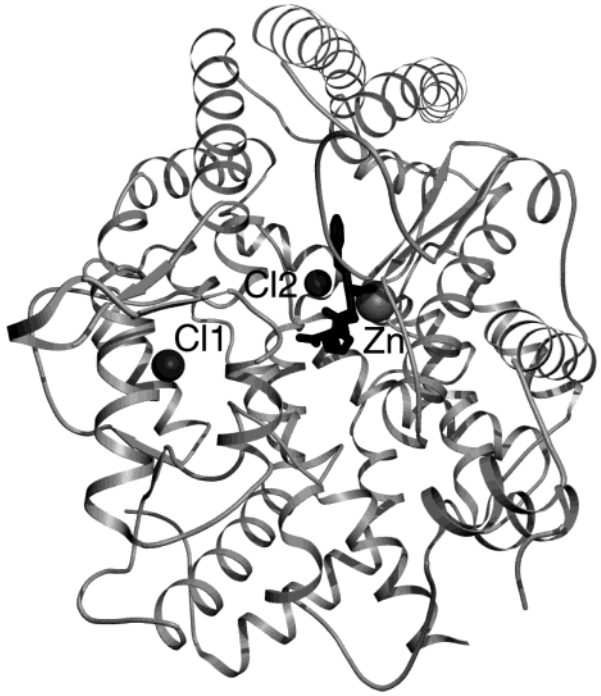


FIGURE 1: Overall topology of the tACE molecule. The active site is indicated by the bound inhibitor lisinopril. The active-site zinc ion and the chloride ions are labeled. The figure was created with MOLSCRIPT (*36*) and rendered with POVRAY (*37*).

whose sequence and 3D structure were elucidated in 1967. Cushman and Ondetti and coworkers (*10*−*12*) speculated that these two metallopeptidases shared a similar catalytic mechanism. Third, the sequences of the bradykinin-potentiating peptides pointed to acyl prolines as likely drug candidates.

In parallel, another approach to ACE inhibitors used rational drug design based on the inhibition of a different zinc proteinase, thermolysin. Two N-carboxyalkyl dipeptides emerged from this search, enalapril and lisinopril, which were approved for marketing in 1985 and 1987, respectively (*13*, *14*). Over the years many more active ACE inhibitors were developed by the pharmaceutical industry, more or less empirically, and 17 are approved for use. Collectively, they serve as the first line of approach to the treatment of hypertension.

Most current ACE inhibitors have a wide range of licensed indications ranging from mild hypertension to post myocardial infarction. For the treatment of hypertension, competing therapeutic approaches also include the use of angiotensin II receptor antagonists and beta-blockers. The continuing burgeoning use of orally active ACE inhibitors in various cardiovascular pathologies underscores the importance of extending these studies, in particular by use of a structure-based drug design approach. Toward this goal, we have recently reported the crystal structure of the human testis ACE (tACE) and its complex with a widely used inhibitor, lisinopril (also known as prinivil and zestril) (*1*). The structure is predominantly composed of α-helices with very few strands and the central active-site groove divides the protein into two subdomains (Figure 1). The lisinopril molecule is buried some 10 Å inside the groove at the active site of the enzyme and directly interacts with the covalently bound $Zn^{2+}$ ion at the bottom of the groove. Apart from the zinc binding motif, the structure is significantly distinct from other well-known metallopeptidases such as bovine carboxypeptidase A and thermolysin, which were thought to have structural similarity with ACE (*1*).

Here we present two new crystal structures of human tACE in complex with the potent inhibitors captopril (generic name capoten) and enalaprilat (generic name vasotec) (Table 1) at 2.0 and 1.82 Å resolution, respectively. We compare these structures with the structure of the lisinopril complex reported recently (*1*). These complexes provide the details of the structural elements that are common in inhibitor binding and help in defining the binding pocket with greater precision that will be useful for the design of better domain-specific inhibitors.

## EXPERIMENTAL PROCEUDRES

*Protein Purification and Crystallization.* A variant of human tACE (tACEΔ36NJ) was expressed in CHO cells and purified to homogeneity, as described previously (*15*). The cocrystals of tACEΔ36NJ with captopril and enalaprilat were grown at 16 °C by the hanging-drop vapor diffusion technique by equilibrating 2 μL of ∼11.5 mg/mL protein solution in 10 mM HEPES and 0.1% PMSF with an equal volume of 10 mM captopril or 10 mM enalapril maleate. The reservoir solution consisted of 15% PEG 4000, 50 mM sodium acetate (pH 4.7), and 10 μM $ZnSO_4$.

*Data Collection and Refinement.* X-ray data for both complexes were collected on station PX 14.1 from a single crystal at cryotemperature (100 K) at the SRS, Daresbury, U.K., by use of an ADSC Quantum 4 CCD detector. All diffraction images were integrated with HKL2000 (*16*). The atomic coordinates of tACE were used as the starting model (PDB code 1O86; *1*). The refinement was carried out with the CNS suite (*17*) and the model building was carried out with O (*18*). Initial model building and refinement was carried out without the inhibitor. In each data set, a set of reflections were kept aside for $R_{free}$ calculation (*19*). The inhibitor and water molecules were modeled by use of both the $2F_o - F_c$ and $F_o - F_c$ SIGMAA weighted maps. The

Table 2: Data Collection and Refinement Statistics for TACE-inhibitor Complexes

| | captopril | enalaprilat |
|---|---|---|
| resolution (Å) | 50−2.0 | 50−1.82 |
| space group (1 mol/au) | $P2_12_12_1$ | $P2_12_12_1$ |
| cell dimension (Å) | 56.65, 84.9, 133.5 | 56.72, 85.35, 133.73 |
| no. of observations | 108 368 | 401 651 |
| no. of unique reflections | 36 760 | 58 651 |
| completeness (%) | 82.8 (78.0)[a] | 99.0 (96.7)[a] |
| $I/\sigma(I)$ | 10.2 (2.9)[a] | 20.9 (4.7)[b] |
| $R_{symm}$[c] | 9.2 (42.8)[a] | 8.9 (40.6)[b] |
| $R_{cryst}$[d]/$R_{free}$[e] | 18.4 (22.7)[a] | 18.8 (21.1)[b] |
| no. of protein atoms | 4671 | 4662 |
| no. of solvent atoms | 430 | 456 |
| no. of inhibitor atoms | 14 | 25 |
| Deviation from Ideality | | |
| bond lengths (Å) | 0.005 | 0.005 |
| bond angles (deg) | 1.2 | 1.2 |
| dihedral angles (deg) | 20.0 | 20.5 |
| improper dihedral (deg) | 0.8 | 0.8 |
| *B*-Factor Statistics (Å$^2$) | | |
| overall *B*-factor | 23.9 | 22.8 |
| protein all atoms | 23.0 | 21.8 |
| protein main chain | 21.9 | 20.5 |
| protein side chain | 24.0 | 23.0 |
| solvent atoms | 32.8 | 33.5 |
| inhibitor atoms | 20.6 | 17.4 |
| $Zn^{2+}$ ion | 17.7 | 15.3 |
| chloride ions Cl1,Cl2 | 14.0, 17.9 | 14.8, 14.3 |

[a] Outermost shell is 2.07−2.0 Å. [b] Outermost shell is 1.89−1.82 Å. [c] $R_{symm} = \Sigma_h\Sigma_i[|I_{i(h)} - \langle I_{(h)}\rangle|]/\Sigma_h\Sigma_i I_{i(h)}$, where $I_{i(h)}$ is the *i*th measurement of reflection *h* and $\langle I_{(h)}\rangle$ is the weighted mean of all measurements of *h*. [d] $R_{cryst} = \Sigma_h|F_o - F_c|/\Sigma_h F_o$, where $F_o$ and $F_c$ are the observed and calculated structure factor amplitudes of reflection *h*. [e] $R_{free}$ is equal to $R_{cryst}$ for a randomly selected 2−3% subset of reflections, which are not used in refinement (*19*).

topology and parameter files for the inhibitors were generated manually and/or by use of the small molecule database Cambridge Structural Database (CSD) from CCDC (*20*). Both the structures have good geometry, and more than 90% of the protein residues are in the most favorable region of the Ramachandran plot. All crystallographic details are listed in Table 2.

## RESULTS AND DISCUSSION

Cocrystallization experiments followed by data collection at the Synchrotron Radiation Source (Daresbury, U.K.) were carried out to determine the structures of captopril− and enalaprilat−tACE to a resolution of 2.0 and 1.82 Å, respectively. Even though the prodrug enalapril maleate was used in the cocrystallization experiment, enalapril (which is the ethyl ester of a long-acting ACE inhibitor enalaprilat) appears to be activated by hydrolysis to enalaprilat in the crystallization medium. The Schechter and Berger nomenclature denotes the positions of the $P_1$, $P_1'$, and $P_2'$ residues of the inhibitors relative to the scissile bond (Figure 2A) (*21*). The overall protein structures of the new inhibitor complexes are predominantly α-helical with a deep inhibitor-binding channel, very similar to the native structure of tACE (Figure 1) (*1*).

*Binding of Captopril.* The competitive tight-binding inhibitor captopril makes a direct interaction with the catalytic $Zn^{2+}$ ion (distance = 2.32 Å, Table 3) deep inside the channel at the active site of tACE (Figure 2B). Similar interactions between the $Zn^{2+}$ ion and captopril have been observed in AnCE, a homologue of tACE from *Drosophila*, in complex with captopril (*22*) as well as in the leukotriene A4 hydrolase−captopril complex (*23*). The zinc coordination by the free sulfhydryl is in contrast to the interaction of the phenyl carboxylate group interaction with the $Zn^{2+}$ ion in the case of the tACE−lisinopril and the tACE−enalaprilat complexes (Figure 2D; *1*). This change to a coordinating sulfhydryl group results in the loss of the positioning hydrogen bond from Tyr 523 present in the other two complexes. Also, the hydrogen bond to the carbonyl group of Ala 354 from the connecting nitrogen between the $P_1$ and $P_1'$ positions is lost. Instead, the captopril is anchored solely at the central carbonyl group and the proline carboxylate group. The central carbonyl group between the sulfhydryl group and the terminal proline is positioned by two strong hydrogen bonds from the two histidines (His 513, 2.69 Å; His 353, 2.54 Å). Similarly, one oxygen of the proline moiety carboxylate group is held by interactions with Tyr 520 (2.66 Å), Gln 281 (3.1 Å), and Lys 511 (2.73 Å). These interactions appear to be sufficient to act as a backstop, positioning the substrate molecule so the carbon of the scissile bond can undergo nucleophilic attack. The other carboxylate oxygen of the proline carboxylate group interacts with the surrounding waters (Figure 2B; Table 3).

*Binding of Enalaprilat.* The interaction of the inhibitor with the protein is more extensive in the tACE−enalaprilat complex than the captopril complex but lacks the contacts with the $S_1'$ pocket present in the lisinopril complex (Figure 2C,D). In the lisinopril complex, the lysyl nitrogen [N3 atom (*1*)], which occupies the deep $S_1'$ pocket, ionically interacts with Glu162 and is associated with Asp 377 via water-mediated interactions. Enalaprilat, on the other hand, has a methyl in the $P_1'$ position. The amino-terminal phenyl moiety of enalaprilat (absent in captopril) is accommodated by a hydrophobic pocket, occupied by Phe 512 and Val 518, and the zinc ion is coordinated by the carboxylate group of enalaprilat (Figure 2C), as in the case of lisinopril.

*Comparison of the Inhibitor Potencies and Observed Interactions.* The ACE inhibitors captopril (C), enalaprilat (E), and lisinopril (L) are highly potent inhibitors of both the N and C domains of somatic ACE and tACE (Table 1). The increase of the $K_i$ values for all three inhibitors for the isolated C domain at 20 mM NaCl compared to those at 300 mM NaCl is approximately 10-fold (*24*). This is in contrast to the isolated N domain, where there is no discernible difference (*24*), and to somatic ACE, where the change in potency at lower chloride concentrations varied markedly with inhibitor (*25*). However, the trend in the relative potencies of these three inhibitors for the C domain (L > E > C) is the same at both low and high chloride concentrations (Table 1) (*24*), suggesting that the chloride-induced conformational change has a uniform effect on the C domain and, therefore also, the tACE binding site. Interestingly, this trend of the relative inhibitor potencies correlates with the number of interactions observed in the crystal complexes with tACE.

Several C-domain active-site residues, of which the only ones that interact with the three inhibitors are located in the $S_1'$ pocket, differ in the corresponding N domain sequence. Among these differences, the exchanges of Glu 162 to Asp 140 and Val 380 to Thr 358 are unlikely to affect the binding of captopril, enalaprilat, or lisinopril. The van der Waals interaction (4.1 Å) of the valine with the C$\beta$ of enalaprilat's

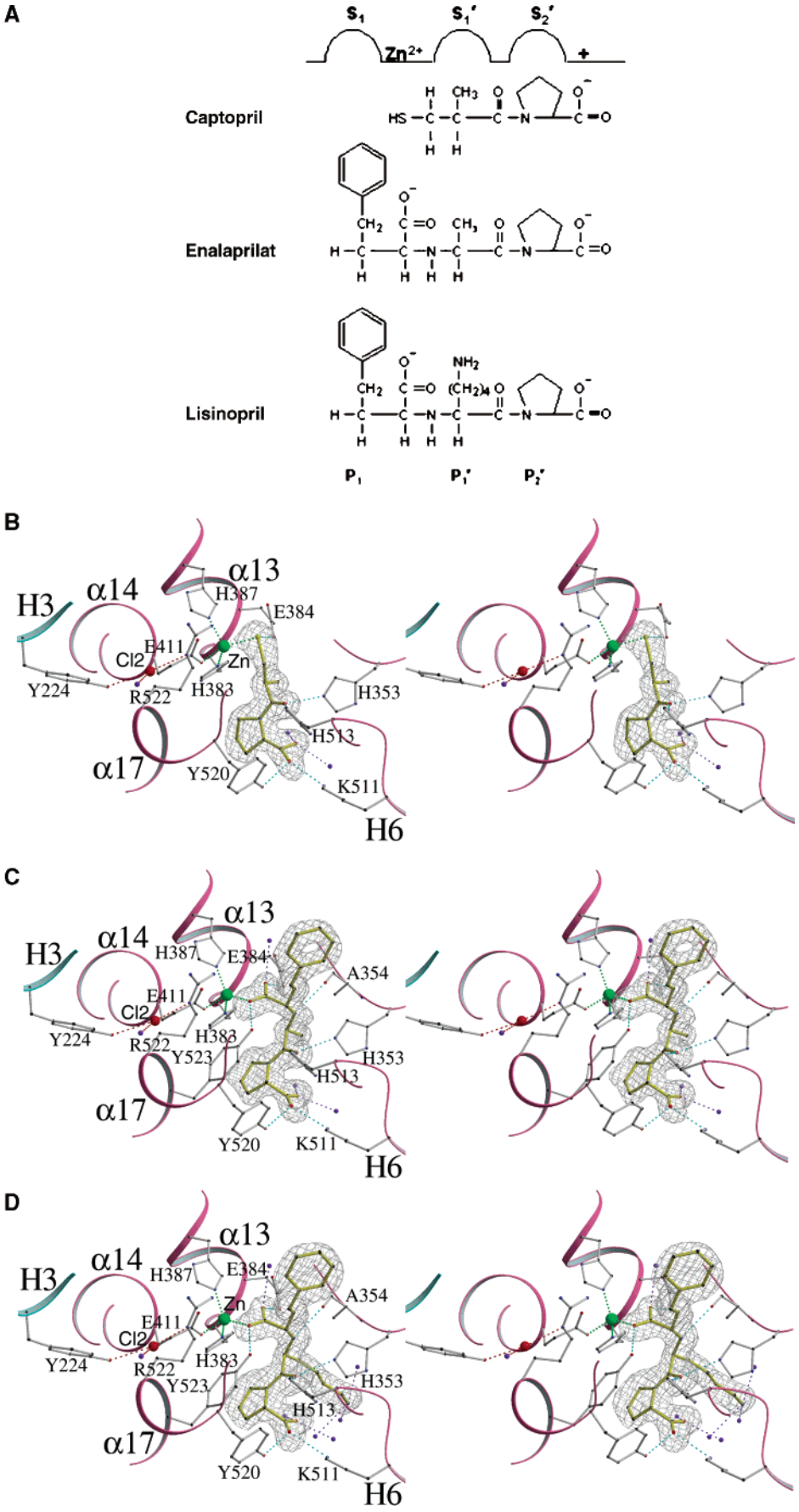


FIGURE 2: (A) Chemical structure of ACE inhibitors captopril, enalaprilat, and lisinopril. (B−D) Stereo representations of interaction for tACE with (B) captopril, (C) enalaprilat, and (D) lisinopril. The electron density map shown is the $F_o - F_c$ map contoured at 3$\sigma$ level. The $Zn^{2+}$ is shown in green, Cl2 in red, inhibitor in yellow, and water in purple. The inhibitor, Cl2, water hydrogen bonds, and zinc coordination are shown with cyan, red, purple, and green dotted lines, respectively. The figure was drawn with MOLSCRIPT and RASTER3D (*36*, *38*).

Table 3: tACE Contacts with (A) Captopril, (B) Enalaprilat, and (C) Lisinopril

| (A) Captopril | | | (B) Enalapril | | | (C) Lisinopril | | |
|---|---|---|---|---|---|---|---|---|
| ligand atoms | interacting atoms | distance (Å) | ligand atoms | interacting atoms | distance (Å) | ligand atoms | interacting atoms | distance (Å) |
| O1 | His 353 NE2 | 2.5 | O1 | His 353 NE2 | 2.7 | O1 | His 353 NE2 | 2.8 |
| S1 | Glu 384 OE2 | 3.1 | N1 | Ala 354 O | 3.0 | N1 | Ala 354 O | 2.9 |
| O2 | Lys 511 NZ | 2.7 | O2 | Glu 384 OE2 | 2.7 | O2 | Glu 384 OE2 | 2.7 |
| O1 | His 513 NE2 | 2.7 | O4 | Lys 511 NZ | 2.8 | O4 | Lys 511 NZ | 2.9 |
| O2 | Tyr 520 OH | 2.7 | O1 | His 513 NE2 | 3.1 | O1 | His 513 NE2 | 3.1 |
| O3 | Wat 759 OH2 | 2.6 | O4 | Tyr 520 OH | 2.6 | O4 | Tyr 520 OH | 2.6 |
| O3 | Wat 866 OH2 | 3.0 | O3 | Tyr 523 OH | 2.8 | O3 | Tyr 523 OH | 2.8 |
| | | | O2 | Wat 747 OH2 | 2.9 | N3 | Glu 162 OE2 | 3.4 |
| | | | O5 | Wat 759 OH2 | 2.7 | O2 | Wat 747 OH2 | 2.8 |
| | | | O5 | Wat 866 OH2 | 2.7 | O5 | Wat 759 OH2 | 2.7 |
| | | | | | | N3 | Wat 787 OH2 | 3.0 |
| | | | | | | N3 | Wat 835 OH2 | 3.3 |
| | | | | | | O5 | Wat 866 OH2 | 2.8 |
| | | | | | | N3 | Wat 1038 OH2 | 3.1 |
| | | | | Cl1 | | | | |
| Cl | Arg 186 NE | 3.2 | Cl | Arg 186 NE | 3.1 | Cl | Arg 186 NE | 3.2 |
| Cl | Arg 186 NH1 | 3.3 | Cl | Arg 186 NH1 | 3.3 | Cl | Arg 186 NH1 | 3.4 |
| Cl | Trp 485 NE1 | 3.3 | Cl | Trp 485 NE1 | 3.3 | Cl | Trp 485 NE1 | 3.3 |
| Cl | Arg 489 NH1 | 3.4 | Cl | Arg 489 NH1 | 3.2 | Cl | Arg 489 NH1 | 3.2 |
| Cl | Wat 755 OH2 | 3.1 | Cl | Wat 755 OH2 | 3.2 | Cl | Wat 755 OH2 | 3.2 |
| | | | | Cl2 | | | | |
| Cl | Arg 522 NE | 3.1 | Cl | Arg 522 NE | 3.3 | Cl | Arg 522 NE | 3.1 |
| Cl | Tyr 224 OH | 3.0 | Cl | Tyr 224 OH | 3.1 | Cl | Tyr 224 OH | 3.0 |
| Cl | Wat 705 OH2 | 3.1 | Cl | Wat 705 OH2 | 3.1 | Cl | Wat 705 OH2 | 3.1 |
| | | | | Zinc | | | | |
| Zn | His 383 NE2 | 2.1 | Zn | His 383 NE2 | 2.1 | Zn | His 383 NE2 | 2.0 |
| Zn | His 387 NE2 | 2.1 | Zn | His 387 NE2 | 2.1 | Zn | His 387 NE2 | 2.1 |
| Zn | Glu 411 OE1 | 2.0 | Zn | Glu 411 OE1 | 1.9 | Zn | Glu 411 OE1 | 2.0 |
| Zn | Cap 702 S1 | 2.3 | Zn | Ena 702 O3 | 2.0 | Zn | Lis 702 O3 | 2.1 |

alanine moiety and lisinopril's lysyl chain are unchanged with the threonine substitution. Furthermore, both glutamate and aspartate would be too distant to make direct interactions with the inhibitors. However, the exchange of Asp 377 for a glutamine in the N domain $S_1'$ pocket, abolishing the ionic interaction with the lysyl nitrogen, might be expected to reduce the potency of lisinopril for the N domain. Furthermore, the longer side chain of the glutamine permits it to occlude the $S_1'$ pocket to a certain extent preventing the accommodation of bulky $P_1'$ groups. The $K_i$ of the N domain for lisinopril is an order of magnitude higher than that for the C domain at both high and low chloride concentrations but is in the same range as that seen for the C domain at low chloride concentration (*24*). This is also true for enalaprilat, which lacks the lysyl moiety and does not interact with this pocket, suggesting that the $S_1'$ pocket may be less important in N-domain interactions or at low chloride concentrations.

The higher affinity of the C domain for lisinopril and enalaprilat contrasts with the higher affinity of the N domain for captopril. Captopril has the same potency for the N domain at both high and low chloride concentrations. However, the $K_i$ for the C domain increases by 1 order of magnitude at high chloride concentrations and 2 orders of magnitude at low chloride concentrations (*24*). The combination of these data suggests that the N domain differs from the C domain such that chloride activation is either reduced or abolished. In addition, its selectivity changes, independent of chloride concentration, such that captopril becomes a better inhibitor than lisinopril or enalaprilat. The modest N-domain selectivity of captopril may, in part, be due to energetic compensations in the active site that are difficult to explain with structural data. Previous studies with the C-domain-specific inhibitor, RXP380, indicate that bulky residues in the $P_1'$ and $P_2'$ positions confer C-domain specificity (*8*), either because the N-domain subsites cannot accommodate them or due to the loss of certain contacts with the exchange of key residues in the C domain (*26*). Moreover as suggested above, the importance of a bulky hydrophobic residue in the $P_2'$ position and its orientation seem to outweigh that of the $P_1'$ residue. However, as captopril and enalaprilat have identical moieties in these positions, the reason for captopril's N-domain specificity remains unclear.

Although comparison of these structures with the available biochemical data on chloride activation and inhibitor potency has allowed some discussion of the trends in inhibitor binding, this analysis remains circumspect. The long history of the study of this enzyme reveals many complexities. In particular, analysis of inhibitor binding and chloride dependence is complicated by the fact that apparent chloride activation is substrate-dependent (*27*, *28*).

*Location of Chloride Ions.* Both chloride ions identified in the tACE structure are located outside the active site (*1*). The first chloride ion, Cl1 (703 Cl), has been speculated to play a role in the stabilization of the enzyme−substrate complex (*29*) even though it is located 20 Å from the zinc ion. The second chloride ion, Cl2 (704 Cl), is located 10.4 Å from the zinc ion and has been shown to be critical for chloride activation (*30*, *31*). Similar interactions between Cl1 and Cl2 and their coordinating ligands were observed in all three ACE−inhibitor complex structures. This fits with the observed biochemical data that suggest that for all three inhibitors the affinity for the C domain decreases proportion-

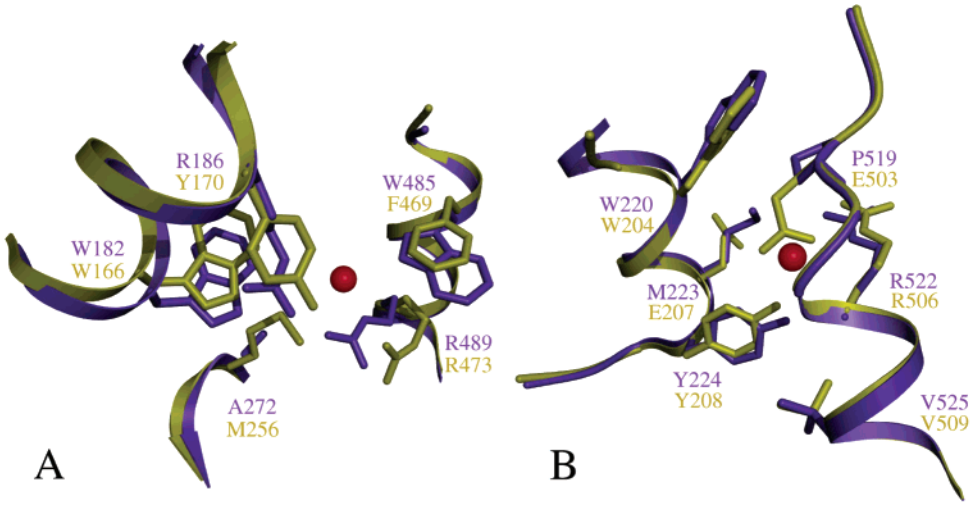


FIGURE 3: Comparison of the residues involved in chloride binding sites 1 (A) and 2 (B) in tACE and their equivalents in AnCE. tACE is shown in purple, AnCE is shown in yellow/green, and the observed chloride ions bound in the tACE structure are shown in red. The figure was drawn with MOLSCRIPT (*36*) and rendered with POVRAY (*37*).

ally at low chloride concentration (*24*) as discussed previously.

Interestingly, no chloride ions were observed in the *Drosophila* AnCE crystal structure (*21*). Although AnCE anion activation is reported to be optimal at 0.8−1.0 M for the substrate Hip-His-Leu (*32*), suggesting that it is less sensitive to chloride ions than mammalian sACE (*27*), it remains poorly characterized. The related insect ACE from *Musca domestica* is activated to a lesser extent than tACE (*33*) but maybe has more in common with the other ACE homologue in *Drosophila*, Acer, which does not undergo chloride activation (*34*). Comparison of the tACE chloride binding sites with the AnCE structure does suggest that AnCE may have a different sensitivity to chloride ions.

The first chloride site, Cl1, shows several differences (Figure 3A). Of the two coordinating arginines at this site, the first (Arg 489 in tACE) is still present in AnCE in a similar position, but the second (Arg 186 in tACE) is replaced by Tyr 170 in AnCE. This substitution creates a binding site more similar to that for Cl2 (704) in tACE as it has only one coordinating arginine paired with a coordinating tyrosine. The change of tryptophan (Trp 485 in tACE), to Phe 469 in AnCE, also prevents the chloride coordination by this residue. Two other notable changes of alanine and valine (Ala 272 and Val 464 in tACE) to methionine (Met 256 and Met 488) at either end of the chloride pocket reduce its size (Val 464 and Met 488, not shown). In particular, Met 256 would appear to narrow the access channel. It is possible, therefore, that these changes may result in a lower affinity site.

The second chloride binding site in tACE, Cl2 (Figure 3B), is much more similar to the equivalent site in AnCE with the exception of Met 223 and Pro 519. Although Met 223 does not coordinate the chloride ion in tACE, its replacement with Glu 207 in AnCE alters both the size and the charge of the pocket. More importantly, however, the change of Pro 519 to the much larger Glu 503 in AnCE appears to block the binding site, suggesting that chloride might not bind to this site. This analysis suggests that, in AnCE, the nature of the Cl1 binding site may be altered and the Cl2 site may be absent. A similar chloride binding pattern was found with the mammalian ACE2 homologue that appears to have only the tACE Cl1 binding site available (*22*) and is reported to be less sensitive to chloride ions, being maximally activated at 1 M NaCl (*35*). It was suggested that a second unresolved chloride exists, but in a different location than tACE, that may help to shift the open/closed conformation of ACE2

## CONCLUSION

The structures of tACE in complex with captopril and enalaprilat, and their comparison with the lisinopril complex, offer detailed insights into inhibitor binding and a definitive picture of the subtle differences in their active-site interactions. Despite the similarity of the N- and C-domain binding pockets, some residues in the $S_1$ and $S_1'$ pockets may contribute toward domain selectivity, a feature that is relevant considering the emergence of the different roles of the two domains. However, the structure of the N domain and/or a chloride-free tACE structure would greatly facilitate our understanding of the available biochemical data. The comparison of tACE with AnCE has also allowed some explanation of possible differences in chloride activation between these two homologous peptidases. In particular, differences in the size of the chloride-binding pocket may play an important role in chloride affinity in the Cl1 site, and the Cl2 site may be absent. Captopril, enalaprilat, and lisinopril were designed without any insight from the three-dimensional structure of ACE but with an assumed mechanistic similarity to carboxypeptidase A. Thus, it is likely that our increased structural knowledge of the ACE binding site will provide a platform for the rational design of new domain-selective ACE inhibitors with improved efficacy and pharmacological profiles.

## ACKNOWLEDGMENT

We thank the staff at Synchrotron Radiation Source, CLRC−Daresbury laboratory (U.K.), for their help during X-ray data collection. We thank Drs. Mario Ehlers and Robert Shapiro for constructive criticism of the manuscript.

## REFERENCES

1. Natesh, R., Schwager, S. L. U., Sturrock, E. D., and Acharya, K. R. (2003) Crystal structure of the human angiotensin-converting enzyme−lisinopril complex, *Nature 421*, 551−554.

2. Ehlers, M. R. W., Fox, E. A., Strydom, D. J., and Riordan, J. F. (1989) Molecular cloning of human testicular angiotensin-converting enzyme: the testis isozyme is identical to the C-terminal half of endothelial angiotensin-converting enzyme, *Proc. Natl. Acad. Sci. U.S.A. 86*, 7741−7745.
3. Turner, A. J., and Hooper, N. M. (2002) The angiotensin-converting enzyme gene family: genomics and pharmacology, *Trends Pharmacol. Sci. 23*, 177−183.
4. Eriksson, U., Danilczyk, U., and Penninger, J. M. (2002) Just the beginning: novel functions for angiotensin-converting enzymes, *Curr. Biol. 12*, R745−752.
5. Acharya, K. R., Sturrock, E. D., Riordan, J. F., and Ehlers, M. R. W. (2003) Ace revisited: A new target for structure-based drug design, *Nat. Drug Discov. 2*, 891−902.
6. Hagaman, J. R., Moyer, J. S., Bachman, E. S., Sibony, M., Magyar, P. L., Welch, J. E., Smithies, O., Krege, J. H., and O'Brien, D. A. (1998) Angiotensin-converting enzyme and male fertility, *Proc. Natl. Acad. Sci. U.S.A. 95*, 2552−2557.
7. Rousseau, A., Michaud, A., Chauvet, M. T., Lenfant, M., and Corvol, P. (1995) The hemoregulatory peptide *N*-acetyl-Ser-Asp-Lys-Pro is a natural and specific substrate of the N-terminal active site of human angiotensin-converting enzyme, *J. Biol. Chem. 270*, 3656−3661.
8. Georgiadis, D., Beau, F., Czarny, B., Cotton, J., Yiotakis, A., and Dive, V. (2003) Roles of the two active sites of somatic angiotensin-converting enzyme in the cleavage of angiotensin I and bradykinin: insights from selective inhibitors, *Circ. Res. 93*, 148−154.
9. Fuchs, S., Xiao, H. D., Cole, J. M., Adams, J. W., Frenzel, K., Michaud, A., Zhao, H., Keshelava, G., Capecchi, M. R., Corvol, P., and Bernstein, K. E. (2004) Role of the N-terminal catalytic domain of ACE investigated by targeted inactivation in mice, *J. Biol. Chem. 279*, 15946−15953.
10. Cushman, D. W., Cheung, H. S., Sabo, E. F., and Ondetti, M. A. (1977) Design of potent competitive inhibitors of angiontensin-converting enzyme. Carboxyalkanoyl and mercaptoalkanoyl amino acids, *Biochemistry 16*, 5484−5491.
11. Ondetti, M. A., Rubin, B., and Cushman, D. W. (1977) Design of specific inhibitors of angiotensin-converting enzyme: new class of orally active antihypertensive agents, *Science 196*, 441−444.
12. Cushman, D. W., and Ondetti, M. A. (1999) Design of angiotensin converting enzyme inhibitors, *Nat. Med. 5*, 1110−1113.
13. Patchett, A. A., Harris, E., Tristram, E. W., Wyvratt, M. J., Wu, M. T., Taub, D., Peterson, E. R., Ikeler, T. J., ten Broeke, J., Payne, L. G., Ondeyka, D. L., Thorsett, E. D., Greenlee, W. J., Lohr, N. S., Hoffsommer, R. D., Joshua, H., Ruyle, W. V., Rothrock, J. W., Aster, S. D., Maycock, A. L., Robinson, F. M., Hirschmann, R., Sweet, C. S., Ulm, E. H., Gross, D. M., Vassil, T. C., and Stone, C. A. (1980) A new class of angiotensin-converting inhibitors, *Nature 288*, 280−283.
14. Patchett, A. A., and Cordes, E. H. (1985) The design and properties of *N*-carboxyalkyldipeptide inhibitors of angiotensin converting enzyme, *Adv. Enzymol. 57*, 1−84.
15. Gordon, K., Redelinghuys, P., Schwager, S. L. U., Ehlers, M. R. W., Papageogiou, A. C., Natesh, R., Acharya, K. R., and Sturrock, E. D. (2003) Deglycosylation, processing and crystallization of human testis angiotensin-converting enzyme, *Biochem. J. 371*, 437−442.
16. Otwinowski, Z., and Minor, W. (1997) Processing of X-ray diffraction data collected in oscillation mode, *Methods Enzymol. 276*, 307−326.
17. Brünger, A. T., Adams, P. D., Clore, G. M., DeLano, W. L., Gros, P., GrosseKunstleve, R. W., Jiang, J. S., Kuszewski, J., Nilges, M., Pannu, N. S., Read, R. J., Rice, L. M., Simonson, T., and Warren, G. L. (1998) Crystallography & NMR system: A new software suite for macromolecular structure determination, *Acta Crystallogr. D54*, 905−921.
18. Jones, T. A., Zou, J. Y., Cowan, S. W., and Kjeldgaard, M. (1991) Improved methods for building models in electron density maps and the location of errors in these models, *Acta Crystallogr. A 47*, 110−119.
19. Brünger, A. T. (1992) Free *R* value: a novel statistical quantity for assessing the accuracy of crystal structures, *Nature 355*, 472−475.
20. Allen, F. H. (2002) The Cambridge Structural Database: a quarter of a million crystal structures and rising, *Acta Crystallogr. B58*, 380−388.
21. Schechter, I., and Berger, A. (1967) On the size of the active site in proteases, *Biochem. Biophys. Res. Commun. 27*, 157−162.
22. Kim, H. M., Shin, D. R., Yoo, O. J., Lee, H., and Lee, J. O. (2003) Crystal structure of *Drosophila* angiotensin I-converting enzyme bound to captopril and lisinopril, *FEBS Lett. 538*, 65−70.
23. Thunnissen, M. M., Andersson, B., Samuelsson, B., Wong, C. H., and Haeggstrom, J. Z. (2002) Crystal structures of leukotriene A4 hydrolase in complex with captopril and two competitive tight-binding inhibitors, *FASEB J. 16*, 1648−1650.
24. Wei, L., Clauser, E., Alhenc-Gelas, F., and Corvol, P. (1992) The two homologous domains of human angiotensin I-converting enzyme interact differently with competitive inhibitors, *J. Biol. Chem. 267*, 13389−13405.
25. Shapiro, R., and Riordan, J. F. (1984) Inhibition of angiotensin converting enzyme: Dependence on chloride, *Biochemistry 23*, 5234−5240.
26. Georgiadis, D., Cuniasse, P., Cotton, J., Yiotakis, A., and Dive, V. (2004) Structural determinants of RXPA380, a potent and highly selective inhibitor of angiotensin-converting enzyme C-domain, *Biochemistry* **2004** (in press).
27. Shapiro, R., Holmquist, B., and Riordan, J. (1983) Anion activation of Angiotensin Converting Enzyme: Dependence on the nature of substrate, *Biochemistry 22*, 3850−3857.
28. Shapiro, R., and Riordan, J. F. (1984) Inhibition of angiotensin converting enzyme: Mechanism and substrate dependence, *Biochemistry 23*, 5225−5233.
29. Tzakos, A. G., Galanis, A. S., Spyroulias, G. A., Cordopatis, P., Manessi-Zoupa, E., and Gerothanassis, I. P. (2003) Structure−function discrimination of the N- and C- catalytic domains of human angiotensin-converting enzyme: implications for $Cl^-$ activation and peptide hydrolysis mechanisms, *Protein Eng. 16*, 993−1003.
30. Bunning, P., and Riordan, J. F. (1983) Activation of angiotensin converting enzyme by monovalent anions, *Biochemistry 22*, 110−116.
31. Liu, X., Fernandez, M., Wouters, M. A., Heyberger, S., and Husain, A. (2001) Arg (1098) is critical for the chloride dependence of human angiotensin I-converting enzyme C-domain catalytic activity, *J. Biol. Chem. 276*, 33518−33525.
32. Williams, T. A., Michaud, A., Houard, X., Chauvet, M. T., Soubrier, F., and Corvol, P. (1996) *Drosophila melanogaster* angiotensin 1-converting enzyme expressed in *Pichia pastoris* resembles the C domain of the mammalian homologue and does not require glycosylation for secretion and enzymatic activity, *Biochem. J. 318*, 125−131.
33. Lamango, N. S., Sajid, M., and Isaac, R. E. (1996) The endopeptidase activity and the activation by $Cl^-$ of angiotensin-converting enzyme from the housefly, *Musca domestica*, *Biochem. J. 314*, 639−646.
34. Houard, X., Williams, T. A., Michaud, A., Dani, P., Isaac, R. E., Shirras, A. D., Coates, D., and Corvol, P. (1998) The *Drosophila melanogaster*-related angiotensin-I-converting enzymes Acer and Ance−distinct enzymic characteristics and alternative expression during pupal development, *Eur. J. Biochem. 257*, 599−606.
35. Vickers, C., Hales, P., Kaushik, V., Dick, L., Gavin, J., Tang, J., Godbout, K., Parsons, T., Baronas, E., Hsieh, F., Acton, S., Patane, M., Nichols, A., and Tummino, P. (2002) Hydrolysis of biological peptides by human angiotensin-converting enzyme-related carboxypeptidase, *J. Biol. Chem. 277*, 14838−14843.
36. Kraulis, P. J. (1991) MOLSCRIPT−A program to produce both detailed & schematic plots of protein structures, *J. Appl. Crystallogr. 24*, 946−950.
37. www.povray.org.
38. Meritt, E. A., and Bacon, D. J. (1997) Raster 3D: photorealistic molecular graphics, *Methods. Enzymol. 277*, 505−524.


BI049480N